High-Temperature Ignition Delay Times and Kinetic Study of Furan

ARTICLE *in* ENERGY & FUELS · APRIL 2012

Impact Factor: 2.79 · DOI: 10.1021/ef300336y

5 AUTHORS, INCLUDING:

Chenglong Tang
Xi'an Jiaotong University
72 PUBLICATIONS **735** CITATIONS
SEE PROFILE

Zuohua Huang
Xi'an Jiaotong University
419 PUBLICATIONS **5,178** CITATIONS
SEE PROFILE

energy&fuels

Article

pubs.acs.org/EF

High-Temperature Ignition Delay Times and Kinetic Study of Furan

Liangjie Wei, Chenglong Tang,* Xingjia Man, Xue Jiang, and Zuohua Huang*

State Key Laboratory of Multiphase Flows in Power Engineering, Xi'an Jiaotong University, Xi'an 710049, People's Republic of China

ABSTRACT: High-temperature ignition delay times of furan were measured behind the reflected shock waves at the elevated pressures (1.2−10.4 atm) for the mixtures with equivalence ratios of 0.5, 1.0, and 2.0 and furan concentrations of 0.25, 0.5 and 1% diluted in argon. An empirical equation was formulated to correlate the measured ignition delay times with the experimental parameters. The measured ignition delay times at 1.2 atm were compared to numerical predictions using a recently developed furan kinetic mechanism (Mech FR), and the results showed that the model yields reasonable agreement with experiments at an equivalence ratio of 2.0 but significant disagreement at the equivalence ratios of 1.0 and 0.5. A modified kinetic model was built by refining rate constants of selected reactions in Mech FR based on the sensitivity analysis results. The modified mechanism yields remarkably better performance in predicting the ignition delay times as well as the thermal decomposition results. Furthermore, the modified mechanism indicates that the most important fuel consumption path is through the unimolecular initiation reaction: furan = FA ($CH_2CCHCHO$), instead of the H abstraction reactions, which were suggested by Mech FR.

1. INTRODUCTION

Recently, biofuel has attracted global research interests because of its renewability and great potential in greenhouse gas reductions.[1] In comparison to the first-generation biofuel (mainly ethanol), furan (C_4H_4O) and its derivatives, such as 2,5-dimethylfuran (DMF) and 2-methylfuran (2-MF), can be produced from nonfood biomass, such as stalks and leaves,[2,3] which does not threaten the food supply and biodiversity.[4] Additionally, furans have a comparable energy density to that of gasoline, which make them more attractive than ethanol. There have already been some investigations on furan-based engines. For example, Thewes et al.[5] studied the in-cylinder spray formation and subsequent evaporation and combustion performance of 2-MF in a direct-injection spark-ignition single-cylinder engine. Their results showed that an engine fueled with 2-MF gave excellent combustion stability, especially under the cold conditions. Ohtomo et al.[6] compared the autoignition and knock properties of furan-based fuels with ethanol, and the results showed that anti-knock ability is improved by 2-MF addition. Zhong et al.[7] performed comparative engine tests with DMF, ethanol, and gasoline in a single-cylinder direct-injection engine. Their results revealed that DMF was a suitable alternative for gasoline because it yields similar or better thermal and emission characteristics than gasoline.

Fundamental combustion data of furans have also been reported. Specifically, Wu et al.[8] measured the laminar flame speed of DMF/air mixtures at elevated pressures. Wu et al.[9] also studied the flame structure of low-pressure premixed DMF/Ar/O_2 mixtures with flame-sampling molecular-beam mass spectrometry techniques. Their measurements show that 2-MF and furan are stable intermediate species in the DMF flames, and they also proposed possible reaction pathways for the consumption of furans. Lifshitz et al. investigated the thermal decomposition of furan,[10] and they proposed that the primary pyrolysis reaction is furan → CH_3CCH + CO, with a rate constant of $k = 10^{15.25 \pm 0.5} \exp[-(77.5 \pm 2.5) \times 10^3/RT]$ s^{-1}. Furthermore, Lifshitz et al. studied the pyrolysis of 2-MF[11] and DMF.[12] They stated that the ring-opening steps for 2-MF and DMF are different from furan. Additionally, the proposed reaction scheme for the pyrolysis of DMF and 2-MF showed a hierarchical similarity that the H radical could substitute the methyl radical of DMF and 2-MF to form 2-MF and furan, respectively. Thus, understanding the combustion chemistry of furan may be the benchmark for accessing the combustion chemistry of the derivatives of furan. Another reason for the combustion chemistry study of furan is that furan is one of the primary structure units of coal, and understanding its combustion chemistry is also important for clean coal combustion.[13] Furthermore, furan is also found to be a major emission from biomass pyrolysis[14] and tobacco smoke.[15]

Most of the previous studies on furan chemistry focused on its thermal decomposition in the shock tube,[10,16] flow reactor,[17] or laser pyrolysis.[18] Besides these experimental studies, furan thermal decomposition kinetics have also been theoretically studied through the quantum chemical methods.[19,20] Intermediate species profiles in low-pressure laminar premixed furan/oxygen/argon flames were measured by Tian et al.[21] with the molecular-beam mass spectrometry technique. They also developed a kinetic mechanism (Mech FR), and the predicted species profiles agree reasonably with the measurements. However, fundamental data, such as laminar flame speed, jet-stirred reactor (JSR) species profiles, and ignition delay times, which have been well-recognized and extensively used for kinetic model validation, have not been reported for furan.

In this study, the shock-tube ignition delay times of furan using the shock tube are presented for the first time. The only available kinetic model of furan is the Mech FR reported in ref 21; thus, its performance is evaluated by comparing the model predicted and the measured ignition delay times. Sensitivity analysis is performed to identify the most important reactions. Refinements to rate constants of selected reactions are

Received: February 27, 2012
Revised: March 30, 2012
Published: April 2, 2012

attempted, and the modified mechanism is subsequently validated against the measured ignition delay times, as well as the previous pyrolysis results.

2. EXPERIMENTAL AND NUMERICAL SPECIFICATIONS

2.1. Experimentations. Experiments were conducted on a shock tube consisting of a 2 m long driver section and a 7.3 m long driven section with a diameter of 11.5 cm. High-purity helium is used as the driver gas. The shock tube is evacuated to the pressure less than 10^{-4} Torr before the experiments. Four fast-response sidewall pressure transducers (PCB 113B26) are located along the end part of the driven section with equal distance (300 mm) apart. An endwall pressure transducer (PCB 113B03) is used to monitor the pressure at the endwall. All of the pressure transducers are shielded with silicone rubbers to minimize the heat-transfer effect. Three time counters (Fluke PM 6690) are used to measure the time intervals between the instants of shock arrival at each pressure transducer location, with which the velocity of the shock wave at the endwall is determined by extrapolating the axial velocity profile to the endwall. Typical attenuation rates of incident shock are less than 3%. The conditions behind the reflected shock wave are calculated by the chemical equilibrium program GasEq,[22] assuming frozen chemistry, with the thermodynamic data suggested by Burcat and Ruscic.[23] Endwall CH* emission is detected at 430 nm with a 10 nm half bandwidth filter by a photomultiplier (Hamamatsu CR 131). The ignition delay time is defined as the time interval between the incident shock wave arrived at the endwall and the onset of ignition, which is defined by extrapolation of the maximum slope line of the CH* emission profile to the baseline,

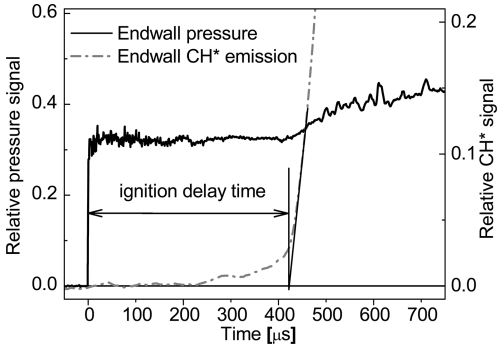

Figure 1. Determination of the ignition delay time (ϕ = 1.0, p = 10.78 atm, and T = 1453 K).

as shown in Figure 1. It can be seen that the onset of ignition definition by CH* emission is consistent with the sharp rise of the endwall pressure. The pressure behind the reflected shock waves is determined by the measured pressure at the endwall. The uncertainty of the temperature behind the reflected shock wave is less than 25 K through the uncertainty analysis. The overall uncertainty of the ignition delay time of the current work is approximately ±10%.

Reactant mixtures were prepared in a 128 L stainless-steel tank. At the room temperature (20 °C), the vapor pressure of furan is 66 kPa[24] and the maximum partial pressure of furan among all test conditions (as shown in Table 1) is less than 2 kPa; thus, there is no fuel condensation influence. The purities of oxygen, argon, and furan are higher than 99.995, 99.995, and 99.5%, respectively.

Table 1. Composition of the Furan/Oxygen/Argon Mixture

mixture	ϕ	fuel (%)	O_2 (%)	Ar (%)
1	0.5	0.25	2.25	97.5
2	1.0	0.50	2.25	97.25
3	2.0	1.00	2.25	96.75

2.2. Kinetic Simulation. Up to now, the only available combustion mechanism for furan is that developed by Tian and co-workers (Mech FR).[21] Mech FR contains 206 species and 1368 reactions and was developed on the basis of their previously reported oxidation mechanism of toluene.[25] Their primary goal for developing Mech FR was to model the burner-stabilized low-pressure premixed-fuel-rich furan flame. Reasonable agreement between the measured and Mech-FR-predicted species profiles was presented. Mech FR was further validated against the measured thermal decomposition results, and fairly good agreement was achieved. It is noted that, while Mech FR was primarily used for modeling the low-pressure flames, Tian and co-workers have nevertheless estimated the rate constants for some pressure-sensitive reactions, such as R1, R2, R51, and R52.

To model the ignition event behind the shock waves and the furan pyrolysis, numerical simulation was conducted using the SENKIN[26] code from the CHEMKIN II package,[27] assuming a zero-dimensional and constant volume adiabatic model. The computed ignition delay time is defined as the time interval between zero and the maximum pressure rise rate point (max dp/dt) in this study.

3. RESULTS AND DISCUSSION

3.1. Ignition Delay Time Measurement. Ignition delay times for furan were measured over a range of experimental conditions: temperatures of 1320−1880 K, pressures of 1.2−10.4 atm, and equivalence ratios of 0.5−2.0. For all test conditions, the oxygen concentration in the fuel/oxygen/argon mixtures is fixed at 2.25%. All of the ignition delay times of the current work are summarized in Table 2. Measured ignition delay times at various test conditions in this work show a strong Arrhenius dependence upon the temperature; thus, an empirical correlation of ignition delay times as a function of experimental parameters was obtained through regression analysis

$$\tau_{ign} = 9.96 \times 10^{-4} \phi^{0.663\pm0.023} p^{-0.684\pm0.015} \exp\left(\frac{41.9 \pm 0.5 \text{ kcal mol}^{-1}}{RT}\right) \quad (1)$$

where τ_{ign} is the ignition delay time in microseconds, R = 1.986 × 10^{-3} kcal mol^{-1} K^{-1} is the universal gas constant, p is the pressure in atm, T is the temperature in kelvin, and ϕ is the equivalence ratio. Typical measured ignition delay times and eq 1 correlation are shown in Figure 2. Increasing in pressure or decreasing in equivalence ratio is found to accelerate the ignition. Figure 3 shows the correlated ignition delay times using eq 1 for all experimental conditions, with a R^2 value of 0.992. Little deviation is observed between the experimental data and eq 1 correlation. However, because of the relatively small range of this study, the eq 1 correlation may not be applied to the conditions in a larger range.

3.2. Numerical Predictions. Figure 4 gives the comparison between the measured ignition delay times and calculated ignition delay times using the Mech FR for furan at p = 1.2 atm and ϕ = 0.5, 1.0, and 2.0. Excellent agreement between the measurements and calculations is presented at an equivalence ratio of 2.0. At an equivalence ratio of 1.0, the calculated ignition delay times at temperatures higher than 1667 K agree reasonably well with the measurements. However, as the temperature is decreased, the calculated ignition delay times using Mech FR are significantly lower than those of measurements and the deviation is increasingly remarkable. This behavior is even more obvious at an equivalence ratio of 0.5. Specifically, at the temperatures of 1671, 1522, and 1414 K, the measured ignition delay times are 188, 616, and 1550 μs,

dx.doi.org/10.1021/ef300336y | Energy Fuels 2012, 26, 2075−2081

Table 2. Measured Furan Ignition Delay Times

ϕ = 0.5, 2.25% O_2			ϕ = 1.0, 2.25% O_2			ϕ = 2.0, 2.25% O_2		
p (atm)	T (K)	τ (μs)	p (atm)	T (K)	τ (μs)	p (atm)	T (K)	τ (μs)
1.20	1414	1550	1.20	1543	709	1.20	1651	461
1.24	1580	357	1.21	1498	1082	1.24	1824	124
1.24	1522	616	1.22	1469	1446	1.24	1882	94
1.24	1484	890	1.22	1610	451	1.25	1559	1082
1.24	1740	107	1.22	1527	832	1.25	1735	229
1.25	1801	71	1.23	1723	161	1.25	1627	560
1.25	1671	188	1.23	1807	86	1.25	1771	186
4.12	1391	896	1.24	1592	532	3.97	1680	168
4.13	1305	1909	1.24	1668	277	4.15	1732	102
4.15	1597	120	1.25	1562	715	4.16	1585	366
4.17	1649	81	1.26	1456	1735	4.17	1668	176
4.20	1536	207	4.10	1621	167	4.19	1516	671
4.21	1430	519	4.16	1490	525	4.25	1474	967
10.32	1558	89	4.17	1378	1823	9.98	1622	142
10.54	1320	984	4.18	1678	111	10.33	1514	381
10.55	1391	442	4.20	1574	280	10.34	1458	655
10.63	1466	227	4.22	1422	1039	10.37	1734	61
			4.24	1732	71	10.39	1588	219
			10.23	1551	154	10.45	1409	902
			10.43	1496	255			
			10.78	1453	427			
			10.95	1461	403			

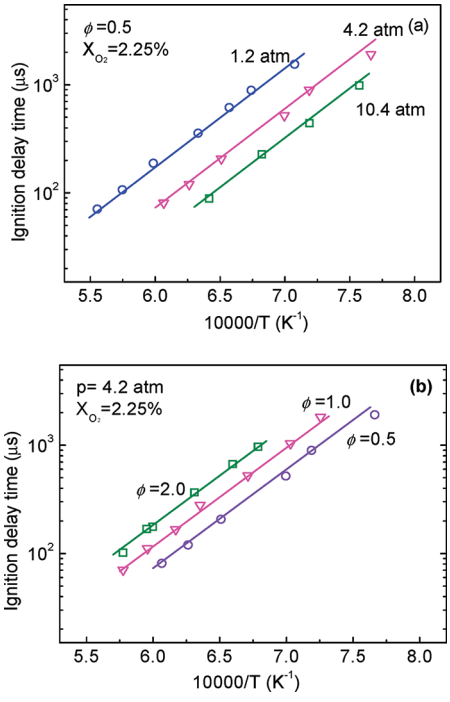

Figure 2. Ignition delay times of the furan/oxygen/argon mixture with (a) different pressures and (b) equivalence ratios. Lines = eq 1.

which are 25, 67, and 180% larger than the numerical predictions, respectively. Comparisons between the predicted ignition delay times using Mech FR and measured ignition delay times under other experimental conditions (which will be presented later) show similar behavior.

Equation 1 shows that the measured ignition delay time exhibits a strong Arrhenius dependence upon the temperature. This Arrhenius dependence is in accordance with almost all other ignition delay times at high temperatures. The fact that

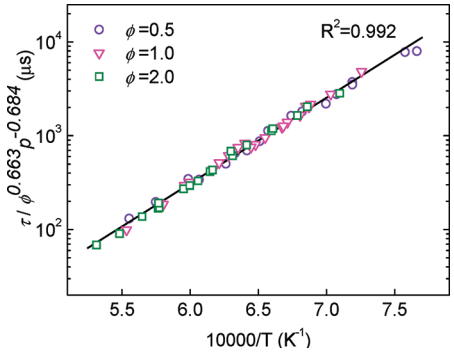

Figure 3. Correlated ignition delay times of furan in the study.

Mech FR fails to show the Arrhenius dependence makes for a further study on the kinetic mechanism of furan.

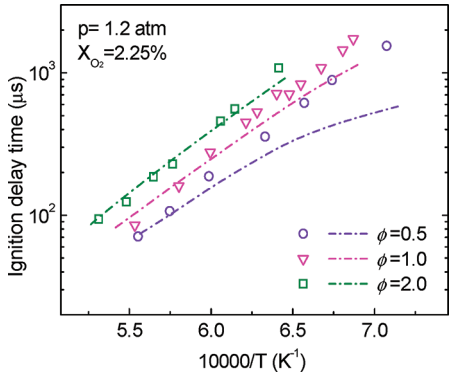

Figure 4. Comparison of furan ignition delay times with Tian's furan mechanism[21] at 1.2 atm (points, measured ignition delay times; dash dot lines, Mech FR predictions).

dx.doi.org/10.1021/ef300336y | *Energy Fuels* 2012, 26, 2075−2081

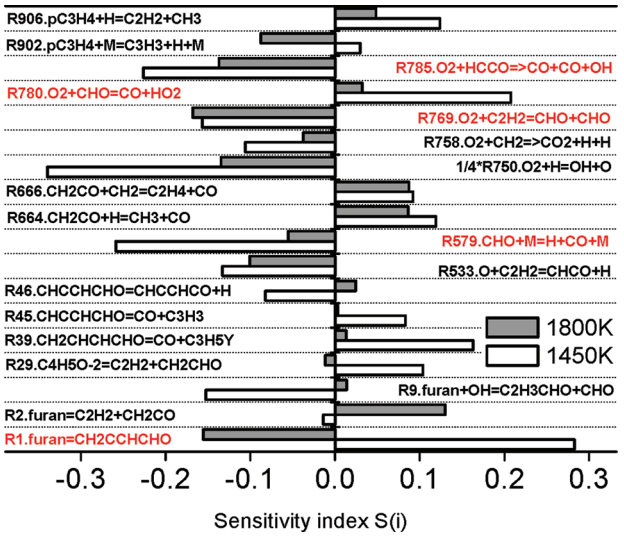

Figure 5. Sensitivity analysis for ϕ = 0.5 and 2.25% O_2 furan/oxygen/argon mixture at 1.2 atm.

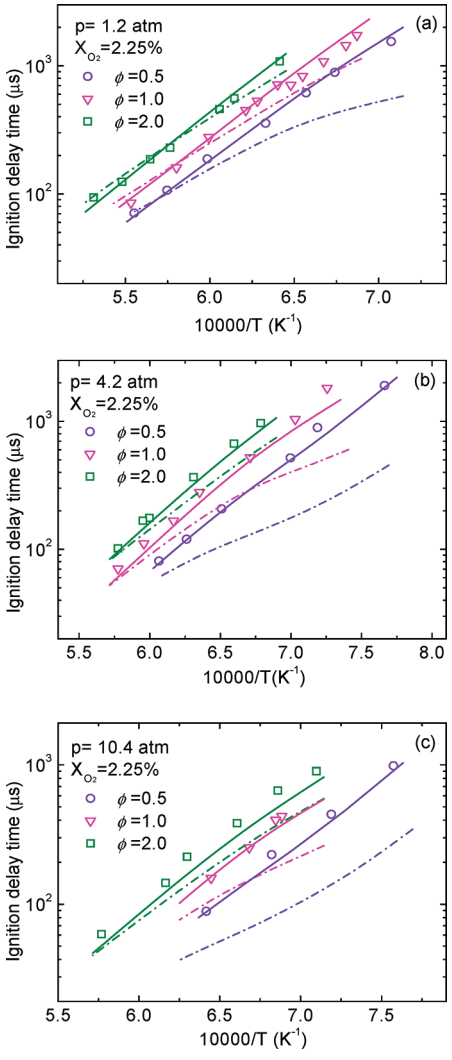

Figure 6. Comparison of experimental data to Tian's mechanism and modified mechanism (dash dot lines, Mech FR; solid lines, Mod_Mech FR).

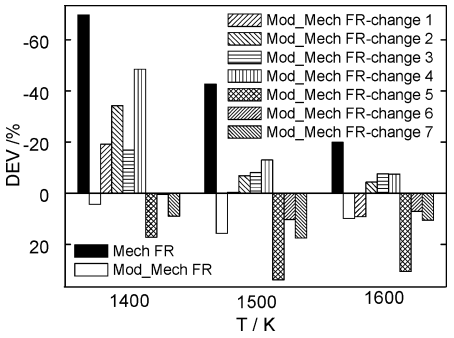

Figure 7. Deviations between predicted and measured ignition delay times for ϕ = 0.5 and 2.25% O_2 furan/oxygen/argon mixture at 1.2 atm.

3.2. Sensitivity Analysis. To ascertain the key reactions in the calculation of ignition delay times, sensitivity analysis was made at the selected conditions using Mech FR. If the rate constants of certain sensitive reactions give large uncertainties, these reactions are regarded for the significant discrepancies between the predicted and measured ignition delay times.

The sensitivity coefficient is calculated by perturbing the reaction rate, defined as

$$S_i = \frac{\Delta\tau_{ign}}{\Delta k_i} / \frac{\tau_{ign}}{k_i} \quad (2)$$

where S_i is the ignition delay time sensitivity, τ_{ign} is the ignition delay time, and k_i is reaction rate of the ith reaction in the mechanism. A negative sensitivity indicates an increase in the forward rate constant of the reaction, resulting in the reduction in τ_{ign}, thus increasing the overall reactivity and vice versa.

Figure 5 depicts the 18 most sensitive reactions on ignition delay time calculations at ϕ = 0.5, p = 1.2 atm, and a temperature of 1450 and 1800 K. As expected, for the temperature range in this study, small radical reactions dominate the autoignition process. The main chain branching reaction R750: O_2 + H = OH + O exhibits an extremely high negative sensitivity coefficient. Reaction R579, which produces H radicals, has a moderately high negative sensitivity coefficient at 1450 K. These two reactions play the most important role in accelerating ignition. Other chain branching reactions, such as R785, R769, and R533, also promote the ignition but are less important. Reactions R780, R39, R29, R906, and R45 have a positive sensitivity coefficient; thus, they act as the several most effective inhibiting reactions, especially at 1450 K. The furan ring open reaction R1 is the most important fuel-specific reaction. It is interesting that the sensitivity of R1 shows a positive index at 1450 K but a negative index at 1800 K. In other words, an increase of the rate constant of R1 may somewhat increase the predicted ignition delay times.

3.3. Optimization on Mech FR. Underprediction of ignition delay times at relatively low temperatures as shown in Figure 4 indicates that Mech FR might have over-/underestimated the rate of certain promotion/inhibition reactions. Thus, we attempted to improve the agreement between the predicted and measured ignition delay times for this condition. Sensitivity analysis in Figure 5 shows that the most important reactions in the ignition delay time calculations are those small radical reactions, such as reactions R750, R780, R785, R769, and R579. Reaction R750 (O_2 + H = OH + O) is perhaps the most important reaction in every hydrocarbon high-temperature oxidation mechanism, and its rate constant is

dx.doi.org/10.1021/ef300336y | Energy Fuels 2012, 26, 2075−2081

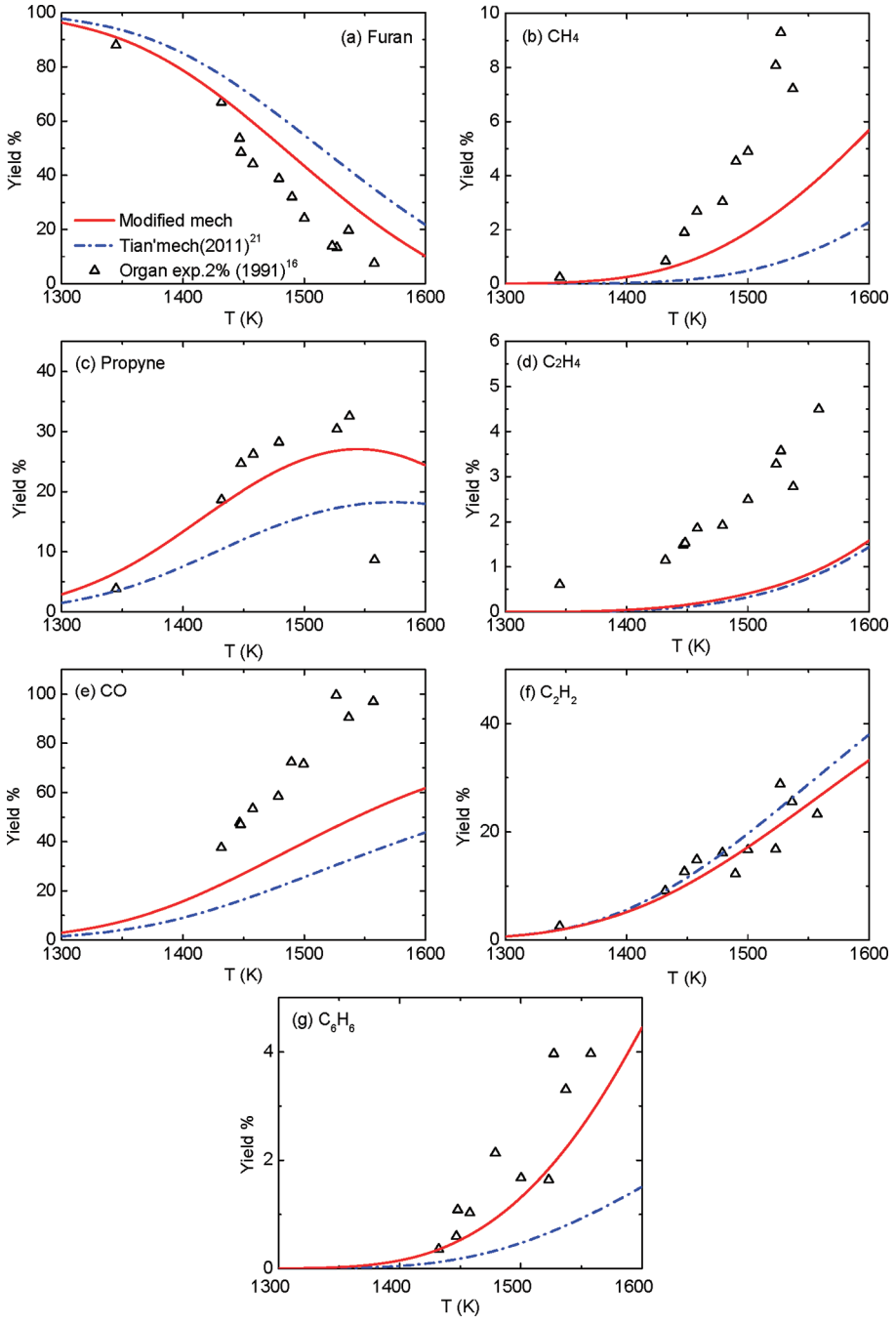

Figure 8. Temperature dependence of designated species in furan pyrolysis (2% furan diluted in argon at 20 atm).

extensively reported that we do not even consider it as a candidate for improving the agreement between Mech FR prediction and measurement. Other small radical reactions (R780, R785, R769, and R579) are comparably less explored, and thus, rate constants of these reactions from different kinetic mechanisms are modified for Mech FR optimization. Additionally, because the fuel-specific reaction R1 has the highest positive sensitivity at 1450 K and the predicted ignition delay times are significantly shorter than the measurement, the rate constants of R1 are artificially magnified by a factor of 2 and better agreement between Mech FR prediction and measured ignition delay times is presented. Furthermore, to modify the methane and benzene prediction for the furan pyrolysis, the rate constants of R17, R18, R900, and R901 are also modified. Details of modifications on Mech FR are summarized as follows: (1) Rate of reaction R1 (furan = $CH_2CCHCHO$) increases by a factor of 2 by doubling the pre-exponential factor. (2) Rate of reaction R579 (CHO + M = H + CO + M) is modified to $4.8 \times 10^{17} T^{-1.2} \exp(-17.73 \text{ kcal mol}^{-1}/RT)$ cm^3 mol^{-1} s^{-1}, as proposed by Hanson et al.[28] (3) Rate of reaction R769 ($O_2 + C_2H_2 = CHO + CHO$) is modified to 3.98×10^{12} $\exp(-28 \text{ kcal mol}^{-1}/RT)$ cm^3 mol^{-1} s^{-1}, as proposed by Pitz et al.[29] (4) Rate of reaction R780 ($O_2 + CHO = CO + HO_2$) is modified to $1.345 \times 10^{13} \exp(-0.4 \text{ kcal mol}^{-1}/RT)$ cm^3 mol^{-1} s^{-1}, as in GRI-Mech 3.0.[30] (5) Rate of reaction R785 (O_2 + HCCO → CO + CO + OH) is modified to 3.2×10^{12} $\exp(-0.854 \text{ kcal mol}^{-1}/RT)$ cm^3 mol^{-1} s^{-1}, as in GRI-Mech 3.0.[30] (6) Rate constant of duplication reactions R900 and

dx.doi.org/10.1021/ef300336y | Energy Fuels 2012, 26, 2075−2081

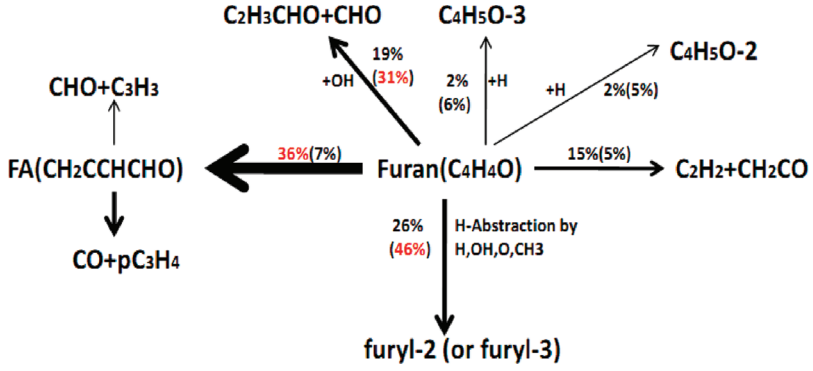

Figure 9. Reaction pathway analysis for furan on the shock tube with the modified mechanism (ϕ = 0.5, 2.25% O_2 furan/oxygen/argon mixture, 10.4 atm, 1450 K, and 20% furan conversion). The percentages in parentheses are the results from the original Mech FR.

R901 ($C_3H_3 + C_3H_3 = C_6C_6$) is modified to one reaction with a constant of 2.0×10^{12} cm^3 mol^{-1} s^{-1}, as proposed by Laskin et al.[31] (7) Rate constants of reactions R17 (furan + CH_3 = furyl-2 + CH_4) and R18 (furan + CH_3 = furyl-3 + CH_4) are modified to 9.6×10^{13} exp(−21 kcal mol^{-1}/RT) cm^3 mol^{-1} s^{-1}, as adopted by Sendt et al.[19]

Figure 6 shows the comparison between the measured and predicted ignition delay times using Mech FR and modified mechanism (Mod_Mech FR) at 1.2, 4.2, and 10.4 atm and at equivalence ratios of 0.5, 1.0, and 2.0. Qualitatively, the predicted ignition delay times with the modified mechanism show better agreements with experiments, and the modified mechanism yields a strong Arrhenius behavior, which is consistent with the measurements in this study and previous literature reports for other fuels at this temperature range. Quantitatively, the modified mechanism shows more close agreement with the measurements under almost all experimental conditions. Specifically, we define a parameter that represents the deviation between mechanism prediction and measured ignition delay times as

$$\mathrm{DEV} = \left(\frac{\tau_{\mathrm{sim}} - \tau_{\mathrm{exp}}}{\tau_{\mathrm{exp}}} \right) \times 100\% \qquad (3)$$

where τ_{sim} and τ_{exp} are the simulated ignition delay time and measured ignition delay time, respectively, and the absolute values of DEV with the Mech FR mechanism at temperatures of 1400, 1500, and 1600 K are 70, 43, and 20%, respectively, while the values of DEV with the Mod_Mech FR mechanism at the same temperatures are minimized to 4, 16, and 10%, respectively, as shown in Figure 7. Additionally, the relative effectiveness from modifying the seven rates of reactions on ignition delay times is illustrated in Figure 7. At 1400 K, the DEV without modifying the rate of R780 in the Mod_Mech FR differs the largest from that of the modified mechanism, which indicates that modification to the rate of reaction R780 (O_2 + CHO = CO + HO_2) is the most effective in the improvement to the agreement between the measured and predicted ignition delay times. At the temperature of 1500 and 1600 K, the most effective is the modification to reaction R785 (O_2 + HCCO → CO + CO + OH).

To further validate the modified mechanism (Mod_Mech FR), comparisons on product profiles of furan pyrolysis between the measured and model predicted are made, as shown in Figure 8. The experimental data use those of Organ and Makie[16] for 2% fuel inlet diluted in argon at a pressure of 20 atm and a residence time of 300 μs on the shock tube. Both predictions from Mech FR and Mod_Mech FR are compared to the experimental data at the temperature range between 1300 and 1600 K. Generally, the modified mechanism (Mod_Mech FR) gives a considerably closer agreement with the measurements than the original Mech FR, specifically for the product concentration profiles of furan, propyne, acetylene, and benzene. Thus, Mod_Mech FR yields good agreement with the measurements. Although Mod_Mech FR and Mech FR underpredict the concentration profiles of CH_4 and CO, Mod_Mech FR gives a closer prediction to measurements than Mech FR. For the product concentration profile of C_2H_4, Mod_Mech FR shows only a slight improvement in the prediction. It is noted that Tian et al.[21] attributed the underprediction of CH_4 to the consumption of the CH_3 radical through reaction R10 (methylfuran + H = furan + CH_3). Additionally, they thought that the underprediction of C_2H_4 resulted from too large of a consumption of the CH_3 radical, which is a key source of C_2H_4. Rate of production (ROP) analysis of C_2H_4 in this study indicates that C_2H_4 is mainly produced through reaction R666: $CH_2CO + CH_2 = C_2H_4 + CO$ and reaction R58: methylfuran = $C_2H_2 + C_2H_4$ + CO.

Figure 9 shows the primary reaction path of furan at 20% fuel conversion for ϕ = 0.5, with an oxygen concentration of 2.25%, p = 10.4 atm, and T = 1450 K. The contributions of each path with Mod_Mech FR (percentages outside the parentheses) and Mech FR (percentages in the parentheses) are above the corresponding arrow. It shows that, in Mech FR, furan is mainly consumed through H abstraction reactions (46%), which generate furly-2 and furly-3 radicals, and the decomposition reaction with OH radical: furan + OH = C_2H_3CHO + CHO (31%). Mod_Mech FR shows that furan is mainly consumed through unimolecular initiations reaction R1: furan = $CH_2CCHCHO$ (36%), while the role of the H abstraction reaction and the decomposition reaction with OH radical to produce C_2H_3CHO are moderated (26 and 19%, respectively).

4. CONCLUDING REMARKS

Ignition delay times of furan were measured behind the reflected shock waves in the temperature range between 1320 and 1880 K and pressure from 1.2 to 10.4 atm for mixtures with equivalence ratios of 0.5, 1.0, and 2.0 and furan concentrations of 0.25, 0.5, and 1% diluted in argon. Main conclusions were summarized as follows: (1) An empirical correlation of ignition delay times as a function of experimental parameters was formulated through multiple regression analysis. (2) Numerical predictions on ignition delay times were subsequently made

dx.doi.org/10.1021/ef300336y | Energy Fuels 2012, 26, 2075−2081

with a recently developed kinetic mechanism of furan (Mech FR) under the selected conditions. Excellent agreement between the measurements and calculations is presented at an equivalence ratio of 2.0. At an equivalence ratio of 1.0, the calculated ignition delay times at temperatures higher than 1667 K agree reasonably well with the measurements. However, as the temperature is decreased, the calculated ignition delay times using Mech FR are significantly lower than those of measurements and the deviation is increasingly remarkable. This behavior is even more obvious at an equivalence ratio of 0.5. (3) A modified furan mechanism (Mod_Mech FR) to Mech FR was developed on the basis of sensitivity analysis. Mod_Mech FR yields a remarkable improvement to the prediction on ignition delay times as well as the product concentration profiles of pyrolysis. (4) Comparisons on primary reaction paths in Mech FR and Mod_Mech FR were made. Mod_Mech FR indicates that the most important fuel consumption path is through the unimolecular initiation reaction: furan = FA ($CH_2CCHCHO$), instead of the H abstraction reactions, which were proposed in Mech FR.

■ AUTHOR INFORMATION

Corresponding Author

*Telephone: 86-29-82665075. Fax: 86-29-82668789. E-mail: chenglongtang@mail.xjtu.edu.cn (C.T.); zhhuang@mail.xjtu.edu.cn (Z.H.).

Notes

The authors declare no competing financial interest.

■ ACKNOWLEDGMENTS

This work was supported by the National Natural Science Foundation of China (51136005 and 51121092). The authors appreciate the helpful discussions with Dr. Z. Tian.

■ REFERENCES

(1) Demirbas, A. Progress and recent trends in biofuels. *Prog. Energy Combust. Sci.* **2007**, *33*, 1−18.

(2) Roman-Leshkov, Y.; Barrett, C. J.; Liu, Z. Y.; Dumesic, J. A. Production of dimethylfuran for liquid fuels from biomass-derived carbohydrates. *Nature* **2007**, *447*, 982−985.

(3) Geilen, F. M. A.; vom Stein, T.; Engendahl, B.; Winterle, S.; Liauw, M. A.; Klankermayer, J.; Leitner, W. Highly selective decarbonylation of 5-(hydroxymethyl)furfural in the presence of compressed carbon dioxide. *Angew. Chem., Int. Ed.* **2011**, *50*, 6831−6834.

(4) Saxena, R. C.; Adhikari, D. K.; Goyal, H. B. Biomass-based energy fuel through biochemical routes: A review. *Renewable Sustainable Energy Rev.* **2009**, *13*, 167−178.

(5) Thewes, M.; Muether, M.; Pischinger, S.; Budde, M.; Brunn, A.; Sehr, A.; Adomeit, P.; Klankermayer, J. Analysis of the impact of 2-methylfuran on mixture formation and combustion in a direct-injection spark-ignition engine. *Energy Fuels* **2011**, *25*, 5549−5561.

(6) Ohtomo, M.; Nishikawa, K.; Suzuoki, T.; Miyagawa, H.; Koike, M. Auto-ignition characteristics of biofuel blends for SI engines. *SAE [Tech. Pap.]* **2011**, DOI: 10.4271/2011-01-1989.

(7) Zhong, S. H.; Daniel, R.; Xu, H.; Zhang, J.; Turner, D.; Wyszynski, M. L.; Richards, P. Combustion and emissions of 2,5-dimethylfuran in a direct-injection spark-ignition engine. *Energy Fuels* **2010**, *24*, 2891−2899.

(8) Wu, X. S.; Huang, Z. H.; Wang, X. G.; Jin, C.; Tang, C. L.; Wei, L. X.; Law, C. K. Laminar burning velocities and flame instabilities of 2,5-dimethylfuran−air mixtures at elevated pressures. *Combust. Flame* **2011**, *158*, 539−546.

(9) Wu, X. S.; Huang, Z. H.; Yuan, T.; Zhang, K. W.; Wei, L. X. Identification of combustion intermediates in a low-pressure premixed laminar 2,5-dimethylfuran/oxygen/argon flame with tunable synchrotron photoionization. *Combust. Flame* **2009**, *156*, 1365−1376.

(10) Lifshitz, A.; Bidani, M.; Bidani, S. Thermal reactions of cyclic ethers at high temperatures. 3. Pyrolysis of furan behind reflected shocks. *J. Phys. Chem.* **1986**, *90*, 5373−5377.

(11) Lifshitz, A.; Tamburu, C.; Shashua, R. Decomposition of 2-methylfuran. Experimental and modeling study. *J. Phys. Chem. A* **1997**, *101*, 1018−1029.

(12) Lifshitz, A.; Tamburu, C.; Shashua, R. Thermal decomposition of 2,5-dimethylfuran. Experimental results and computer modeling. *J. Phys. Chem. A* **1998**, *102*, 10655−10670.

(13) Meyers, R. A.; Attar, A. *Coal Structure*; Academic Press: New York, 1982.

(14) Rice, R. W.; Sanyal, A. K.; Elrod, A. C.; Bata, R. M. Exhaust gas emissions of butanol, ethanol, and methanol−gasoline blends. *J. Eng. Gas Turbines Power* **1991**, *113*, 377−381.

(15) Holzer, G.; Oró, J.; Bertsch, W. Gas chromatographic−mass spectrometric evaluation of exhaled tobacco smoke. *J. Chromatogr., A* **1976**, *126*, 771−785.

(16) Organ, P. P.; Mackie, J. C. Kinetics of pyrolysis of furan. *J. Chem. Soc., Faraday Trans.* **1991**, *87*, 815−823.

(17) Grela, M. A.; Amorebieta, V. T.; Colussi, A. J. Very low-pressure pyrolysis of furan, 2-methylfuran, and 2,5-dimethylfuran—The stability of the furan ring. *J. Phys. Chem.* **1985**, *89*, 38−41.

(18) Hore, N. R.; Russell, D. K. The thermal decomposition of 5-membered rings: A laser pyrolysis study. *New J. Chem.* **2004**, *28*, 606−613.

(19) Sendt, K.; Bacskay, G. B.; Mackie, J. C. Pyrolysis of furan: *Ab inito* quantum chemical and kinetic modeling studies. *J. Phys. Chem. A* **2000**, *104*, 1861−1875.

(20) Liu, R.; Zhou, X.; Zuo, T. The pyrolysis mechanism of furan revisited. *Chem. Phys. Lett.* **2000**, *325*, 457−464.

(21) Tian, Z.; Yuan, T.; Fournet, R.; Glaude, P.-A.; Sirjean, B.; Battin-Leclerc, F.; Zhang, K.; Qi, F. An experimental and kinetic investigation of premixed furan/oxygen/argon flames. *Combust. Flame* **2011**, *158*, 756−773.

(22) Morley, C. *Gaseq*; http://www.c.morley.dsl.pipex.com/ (accessed Aug 2010).

(23) Burcat, A.; Ruscic, B. *Third Millennium Ideal Gas and Condensed Phase Thermochemical Database for Combustion with Updates from Active Thermochemical Tables*; http://garfield.chem.elte.hu/Burcat/burcat.html (accessed Nov 2010).

(24) Speight, J. G.; Lange, N. A. *Lange's Handbook of Chemistry*; McGraw-Hill: New York, 2005.

(25) Tian, Z.; Pitz, W. J.; Fournet, R.; Glaude, P.-A.; Battin-Leclerc, F. A detailed kinetic modeling study of toluene oxidation in a premixed laminar flame. *Proc. Combust. Inst.* **2011**, *33*, 233−241.

(26) Lutz, A. E.; Kee, R. J.; Miller, J. A. *SENKIN: A Fortran Program for Predicting Homogeneous Gas Phase Chemical Kinetics with Sensitivity Analysis*; Sandia National Laboratories: Albuquerque, NM, 1988; SAND87-8248.

(27) Kee, R. J.; Rupley, F. M.; Miller, J. A. *CHEMKIN-II: A FORTRAN Chemical Kinetics Package for the Analysis of Gas-Phase Chemical Kinetics*; Sandia National Laboratories: Albuquerque, NM, 1989; SAND89-8009B.

(28) Friedrichs, G.; Herbon, J. T.; Davidson, D. F.; Hanson, R. K. Quantitative detection of HCO behind shock waves: The thermal decomposition of HCO. *Phys. Chem. Chem. Phys.* **2002**, *4*, 5778−5788.

(29) Pitz, W. J.; Westbrook, C. K. Chemical kinetics of the high pressure oxidation of *n*-butane and its relation to engine knock. *Combust. Flame* **1986**, *63*, 113−133.

(30) Smith, G. P.; Golden, D. M.; Frenklach, M.; Moriarty, N. W.; Eiteneer, B.; Goldenberg, M.; Bowman, C. T.; Hanson, R. K.; Song, S.; Gardiner, W. C., Jr.; Lissianski, V. V.; Qin, Z. *GRI-Mech 3.0*; http://www.me.berkeley.edu/gri_mech/ (accessed Nov 2010).

(31) Laskin, A.; Wang, H.; Law, C. K. Detailed kinetic modeling of 1,3-butadiene oxidation at high temperatures. *Int. J. Chem. Kinet.* **2000**, *32*, 589−614.